Electrochemical and Complexation Studies of Ferrocenyl Complexes Bearing Terpyridine or Phenanthroline Ligands

Jean-Claude Moutet,*[a] Eric Saint-Aman,[a] Guy Royal,[a] Sophie Tingry,[a][‡] and Raymond Ziessel[b]

Keywords: N ligands / Sandwich complexes / Receptors / Cyclic voltammetry

The coordinative properties of 1,1′-bis(phen)- and bis(terpy)-carboxyester-bridged derivatives of ferrocene L^1 and L^2 (phen refers to 2,9-substituted-1,10-phenanthroline; terpy refers to 4′-substituted-2,2′:6′,2"-terpyridine) towards various transition metal cations have been investigated by a combination of cyclic voltammetry, mass spectrometry and ^1H NMR spectroscopy. These novel redox receptors form 1:1 ligand:metal complexes with all the surveyed metal cations (L^1: M = Cu^I, Ni^{II}, Fe^{II}, Hg^{II}; L^2: M = Ni^{II}, Fe^{II}, Hg^{II}). Particular attention was paid to the recognition properties of these redox-active ligands, as monitored by the modulation of the potential of the ferrocene/ferricinium (Fc/Fc^+) couple upon complexation. Complexation of L^1 gives rise to a new emerging Fc/Fc^+ redox peak system. In contrast, complexation of L^2 does not alter this redox process appreciably. In addition, decomposition of free L^2 occurs upon oxidation and causes the growth of a film of an Fe-bis(terpy) complex onto the electrode surface.

Introduction

Molecular structures comprising two or more coordinated metal cations are useful models for studying electronic coupling between metal centers in different oxidation states and for the coupling of a remote active metal centre to a putative catalytic site.[1] Ferrocenyl units are frequently employed as redox-active sites in supramolecular assemblies,[2] owing to their well-behaved redox activity as well as their synthetic versatility. A number of ferrocenyl-functionalized bipyridines,[3] terpyridines,[3c,4] quinquepyridines,[5] and sexipyridines[6] have been synthesized for these reasons.

In previous studies,[7] we reported that mono(bipy)- and bis(bipy)ester- and -carboxamide-bridged derivatives of ferrocene (bipy = 2,2′-bipyridine) present a very rich coordination chemistry and electrochemistry in the presence of various transition metal cations. The resultant di-, tri-,or tetranuclear complexes displayed significant levels of electronic coupling between the metal sites. Additionally, it was demonstrated that these redox ligands can be used for the electrochemical recognition of certain transition metal cations in both homogeneous[7a][7d] and polymeric[7b] phases by way of a large shift in the ferrocene/ferricinium (Fc/Fc^+) redox couple following the binding of a guest cation at the coordination site. Here we report on the electrochemical response of novel 1,1′-bis(phenanthroline) and bis(terpyridine) derivatives of ferrocene L^1 and L^2 (Figure 1) to various transition metal cations. Some particular spectral properties (^1H NMR, FT IR and electronic absorption spectra) of certain complexes are also described.

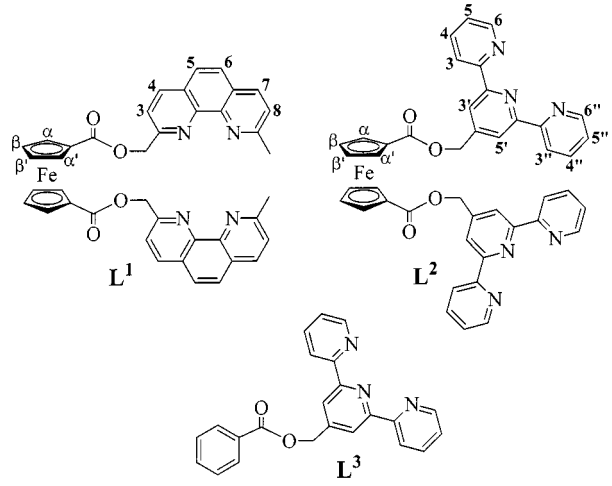

Figure 1. Chemical formula of ligands L^1, L^2 and L^3

Results and Discussion

Complexation of L^1 with Cu^I, Ni^{II}, Fe^{II} and Hg^{II}

The cyclic voltammetry (CV) curve for the free ferrocene-bis(phenanthroline) ligand L^1 in CH_3CN solution is characterized by a re-

[a] Laboratoire d′Electrochimie Organique et de Photochimie Rédox, UMR CNRS 5630, Université Joseph Fourier Grenoble 1,
BP 53, 38041 Grenoble Cédex 9, France
[b] Laboratoire de Chimie, d′Electronique et de Photonique Moléculaires, Ecole de Chimie, Matériaux et Polymères, Université Louis Pasteur,
25 rue Becquerel, 67087 Strasbourg Cédex 02, France
[‡] Current address: LMPM, UMR CNRS 5635,
1919 route de Mende, 34293 Montpellier Cédex 5, France

  1434−1948/02/0303−0692 $ 17.50+.50/0 *Eur. J. Inorg. Chem.* **2002**, 692−698

versible, one-electron wave corresponding to the Fc/Fc^+ couple ($E_{1/2}$ = 0.58 V; labeled I in Figure 2A and 2C, curves a). We have examined how complexation of L^1 by various transition metal cations (Cu^I, Ni^{II}, Fe^{II}, and Hg^{II}) affects the electrochemical features of the ferrocene centre. Metal cations were added as the salts $[Cu(CH_3CN)_4]ClO_4$, $[Ni(ClO_4)_2]$, $[Fe(ClO_4)_2]$ or $[Hg(CF_3SO_3)_2]$. The electrochemical data for L^1 and its metal complexes are summarized in Table 1.

Cu^IL^1 and $Ni^{II}L^1$ Complexes

The electrochemical behavior of L^1 in the presence of Cu^I and Ni^{II} ions is similar to that already observed with ferrocenyl receptors containing 2,2′-bipyridine ligands.[7] The progressive complexation of L^1 causes the emergence of a new redox peak system corresponding to the complexed Fc/Fc^+ redox couple (labeled II on Figure 2) at the expense of the original Fc/Fc^+ wave for the free ligand. It should be emphasized that oxidation of the ferrocene group occurs in the $[Cu^{II}L^1]^{2+}$ complex (see below). The new wave reaches full development at a metal cation:L^1 ratio of 1 (Figure 2A and 2C, curves c). These observations are in keeping with

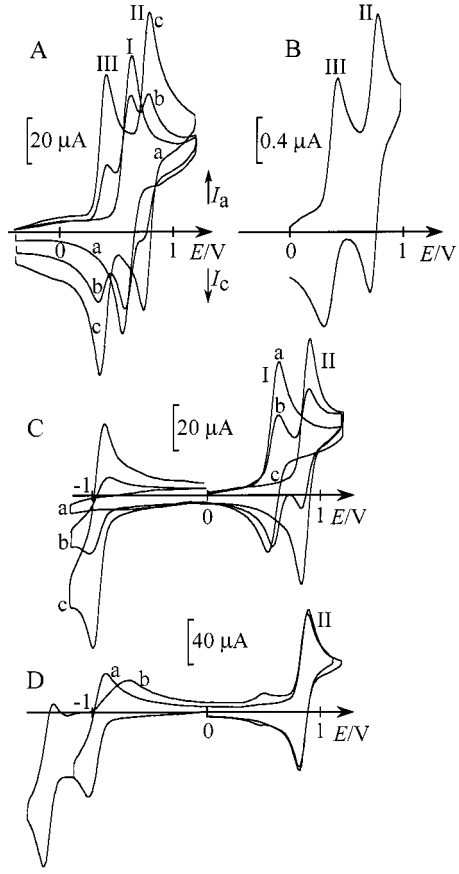

Figure 2. Cyclic voltammograms in CH_3CN + TBAP 0.1 M; (A): (a) free L^1 (2.9 mM), (b) L^1 + 0.4 $[Cu(CH_3CN)_4]ClO_4$, (c) L^1 + 1.0 $[Cu(CH_3CN)_4]ClO_4$, Pt disk (5 mm diameter); (B) $[CuL^1](ClO_4)$ 1 mM at a C disk (3 mm diameter); (C) (a) free L^1 (1.5 mM), (b) L^1 + 0.4 $Ni(ClO_4)_2$, (c) L^1 + 1.0 $Ni(ClO_4)_2$, Pt disk (5 mm diameter); (D) $[Ni\ L^1](ClO_4)_2$ 1 mM at a Pt disk (5 mm diameter); scan rate 0.1 Vs^{-1}

Table 1. Cyclic voltammetric data[a] for $[ML^1]$ complexes with M = Cu^I, Ni^{II}, Fe^{II}, Hg^{II}

Metal	Fc/Fc^+	Metal−centered redox systems
Free L^1	0.58	
Cu^I	0.74[b]	0.33($Cu^{I/II}$)
Ni^{II}	0.86	−0.96($Ni^{II/I}$),[c] −1.39($Ni^{I/0}$)[c] [d]
Fe^{II}	0.85	1.31($Fe^{II/III}$),[e] −1.33($Fe^{II/I}$)[c,e]
Hg^{II}	0.68	−0.75($Hg^{II/I}$)[c,e]

[a] $E_{1/2}$, V vs. $Ag/AgNO_3$ 0.01 M in CH_3CN + TBAP 0.1 M, determined by CV on Pt in CH_3CN + TBAP 0.1 M; ν = 0.1 Vs^{-1}. [b] Ferrocene oxidation occurs after copper oxidation, i.e. in the $[Cu^{II}L^1]^{2+}$ complex.[c] Formal oxidation states. [d] Poorly reversible system. [e] E_p; irreversible peak.

the formation of 1:1 $[CuL^1]^+$ and $[NiL^1]^{2+}$ complexes. This result is corroborated by electrochemical studies carried out with genuine samples of pure $[CuL^1](ClO_4)$ (Figure 2B) and $[NiL^1](ClO_4)_2$ (Figure 2D) complexes: when solubilized in CH_3CN + TBAP solution they display the same CV features as obtained by in situ complexation of L^1 with one mol equivalent of Cu^I (Figure 2A, curve c) or Ni^{II} (Figure 2C, curve c).

Complexation of L^1 with Cu^I causes the rise of a new redox peak system ($E_{1/2}$ = 0.33 V) attributed to the complexed Cu^I/Cu^{II} couple (labeled III on Figure 2A and 2B). The relatively high redox potential of the $Cu^{I/II}$ redox system is in good agreement with those previously reported for various polypyridyl copper complexes.[7a,8] The electrochemical behavior of $[CuL^1]^+$ is summarized in Equation (1):

$$[Cu^I\mathbf{L^1}]^+ \underset{+e}{\overset{0.33\ V\ -e}{\rightleftharpoons}} [Cu^{II}\mathbf{L^1}]^{2+} \underset{+e}{\overset{0.74\ V\ -e}{\rightleftharpoons}} [Cu^{II}(\mathbf{L^1})^+]^{3+} \quad (1)$$

Complexation of L^1 with Ni^{II} ions is also revealed by the appearance of two reversible one-electron reduction waves at −0.96 V and −1.39 V (Figure 2C and 2D). This behavior is reminiscent of that of the Ni^{II} complex of the 2,9-di-*p*-anisyl-1,10-phenanthroline.[8] However, the reduced $[NiL^1]^+$ complex is less stable, since the $Ni^{II/I}$ redox couple was found at a notably less negative potential in the nickel bis-(anisylphenanthroline) complex ($E_{1/2}$ = −0.18 V vs. SCE).[8] Furthermore, the second reduction of the nickel complex down to its $[NiL^1]^0$ form leads to some decomplexation, as shown by the appearance on the reverse scan of a weak Fc/Fc^+ peak system corresponding to the free ligand (Figure 2D, curve b). The redox behavior of $[NiL^1]^{2+}$ is summarized in Equation (2).

$$[Ni^0\mathbf{L^1}]^0 \underset{+e}{\overset{-1.39\ V\ -e}{\rightleftharpoons}} [Ni^I\mathbf{L^1}]^+ \underset{+e}{\overset{-0.96\ V\ -e}{\rightleftharpoons}} [Ni^{II}\mathbf{L^{1\bullet}}]^{2+} \underset{+e}{\overset{0.86\ V\ -e}{\rightleftharpoons}} [Ni^{II}(\mathbf{L^1})^+]^{3+} \quad (2)$$

Complexation of L^1 by Cu^I was further investigated by ^1H NMR titration. Addition of Cu^I cation to a solution of L^1 in CD_3CN produced significant perturbations in all ^1H

NMR resonances recorded at 273 K. Signals for both free and complexed ligand were observed at a substoichiometric level of copper salt. This fact reveals the inertness of this complex, i.e. intramolecular exchange is restricted on the NMR time scale. The ^{1}H NMR spectrum shows only resonances for the copper complex after the addition of one mol equivalent of Cu^I ions. In the copper complex, all the resonances of protons at the phenanthroline rings are shifted downfield (see the Experimental Section). As noticed in copper complexes of 1,1′-(bispyridyl) ferrocenes,[7a] ferrocene-proton pairs become nonequivalent in the $[CuL^1]^+$ complex; the α′-Cp resonances at δ = 4.91 in the free ligand are shifted upfield to δ = 4.72, whereas the α-Cp signal is found at δ = 3.66. The signal of the methylene protons changes from a singlet (δ = 5.52 in free L^1) to an AB system (H-exo: δ = 5.47, J = 12.0 Hz; H-endo: δ = 4.88, J = 12.0 Hz). The prochirality of the methylene protons is consistent with the fact that the 1,10-phenanthroline arms become more rigid upon coordination.

$Fe^{II}L^1$ Complex

Very recently,[7c] we found that L^1 forms a high spin 1:1 complex $[FeL^1]^{2+}$ with Fe^{II} ions. This unusual stoichiometry (two phen ligands per iron centre) was unambiguously established by FAB-MS data and X-ray structure analysis. The crystal structure of the complex revealed that the iron(II) coordination environment consists of four nitrogen atoms provided by the phenanthroline units and two oxygen atoms of the carbonyl groups, forming a distorted octahedral environment.

CV experiments show that the progressive complexation of L^1 with Fe^{II} ions leads to the growth of a new Fc/Fc^+ redox wave ($E_{1/2}$ = 0.85 V) at the expense of the original wave for free L^1 (Figure 3). However a weak oxidation peak for the uncomplexed ligand (labeled with an asterisk in Figure 3) is always seen even in the presence of an excess (e.g. 1.2 equivalent) of Fe^{II} ions. Obviously, the $[FeL^1]^{2+}$ complex is weaker than the copper and nickel complexes. Furthermore, oxidation of the ferrocene centre in the iron complex leads to partial decomplexation, as shown by the appearance on the reverse scan of a large reduction peak corresponding to the Fc/Fc^+ redox system in the free ligand (labeled with a double asterisk in Figure 3). Complexation of L^1 with Fe^{II} also gives rise to an irreversible oxidation wave (E_p = 1.31 V) at more positive potentials corresponding to the $Fe^{II/III}$ redox process in the $[FeL^1]^{2+}$ complex (Figure 3, curve b). The redox behavior of $[FeL^1]^{2+}$ is summarized in Equation (3).

$$[Fe^{II}(\mathbf{L^1})^-]^+ \xleftarrow[+e]{-1.33\ V} [Fe^{II}\mathbf{L^1}]^{2+} \underset{+e}{\overset{0.85\ V\ -e}{\rightleftharpoons}} [Fe^{II}(\mathbf{L^1})^+]^{3+} \xrightarrow[-e]{1.31\ V} [Fe^{III}(\mathbf{L^1})^+]^{4+} \quad (3)$$

The $Fe^{II/III}$ redox process in the $[FeL^1]^{2+}$ complex occurs at a potential close to that of free Fe^{2+} cations. In the presence of an excess of Fe^{II}, this last process (E_p = 1.44 V) is seen on the CV curve as a shoulder that appears at the positive foot of the complexed $Fe^{II/III}$ redox peak (Figure 3, curve b). The abnormally high intensity of the oxidation peak corresponding to the $Fe^{II/III}$ redox process in the $[FeL^1]^{2+}$ complex is probably due to its overlapping with the background current corresponding to some electrolyte oxidation that occurs at this potential. By comparing $[Fe^{II}L^1]^{2+}$ to a regular $[Fe(phen)_3]^{2+}$ complex (phen = 5,6-dimethyl-1,10-phenanthroline, for example; $E_{1/2}[Fe^{II/III}]$ = 0.62 V), it is obvious that the unusual coordination environment in the $[FeL^1]^{2+}$ complex strongly stabilizes the divalent state of the iron centre. It should be noted that stabilization of the Fe^{II} state in the $[Fe^{II}L^1]^{2+}$ complex based on phen binding sites is larger than in the corresponding Fe-bis(bipy) derivative of ferrocene ($E_{1/2}$ = 0.99 V).[7c]

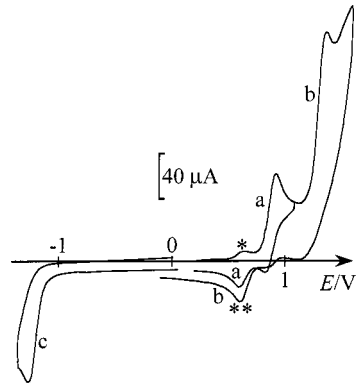

Figure 3. Cyclic voltammograms in CH_3CN + TBAP 0.1 M at a Pt disk electrode (5 mm diameter) of L^1 (2 mM) + 1.2 $Fe(ClO_4)_2$: (a) scan between 0 and 1 V; (b) scan between 0 and 1.5 V; (c) scan between 0 and −1.2 V; scan rate 0.1 Vs^{-1}

Oxidation of the iron centre in the $[Fe^{II}(L^1)^+]^{3+}$ complex (Figure 3, curve b) leads to an important degradation; on the reverse scan the complexed Fc/Fc^+ redox couple becomes less reversible and the intensity of the free Fc^+ reduction wave is twice that observed when the CV scan is restricted to the 0 to 1 V potential range. Since the iron-centered oxidation occurs after that of the ferrocenyl unit, decomplexation probably results from strong repulsive electrostatic forces between the Fc^+ and Fe^{III} centers in the fully oxidized $[Fe^{III}(L^1)^+]^{4+}$ complex.

CV curves recorded in the negative-potential region show a number of ill-behaved, irreversible reduction peaks between −1 V and −2 V; the first one appears at E_p = −1.33 V (Figure 3, curve c). Once again, the behavior of $[FeL^1]^{2+}$ contrasts with that for a regular Fe-tri(phen) complex, which is characterized by three ligand-centered, reversible reduction waves ($E_{1/2}$ = −1.85, −2.03, −2.25 V; phen = 5,6-dimethyl-1,10-phenanthroline).

$Hg^{II}L^1$ Complex

A mercury(II) complex was obtained from L^1 upon treatment with $Hg(CF_3SO_3)_2$. The FAB-mass spectra were identical when the complex was prepared using one or two molar equivalents of mercury salt and clearly show a 1:1 stoichiometry.

When investigated by NMR spectrometry, the progressive addition of Hg^{II} cations to a solution of L^1 in CD_3CN produces significant perturbations in all ^1H NMR resonances recorded at room temperature. The spectra are characterized by broad, unstructured peaks until one mol equivalent of metal cation had been added. The NMR spectra remained unresolved over the −20 °C to 40 °C temperature range and the solutions were EPR silent. These observations reveal that the intermolecular exchange is fast on the NMR time scale at substoichiometric levels of mercury salt. After the addition of more than one mol equivalent of Hg^{II} cations, well-behaved NMR signals for the Hg^{II} complex develop. As already noticed for the $[CuL^1]^+$ complex, the ferrocene-proton pairs become nonequivalent. The α-Cp and α′-Cp resonances are shifted downfield and upfield, respectively. The NMR signal of the methylene protons changes from a singlet to an AB system (see Figure 4 and the Exp. Sect.).

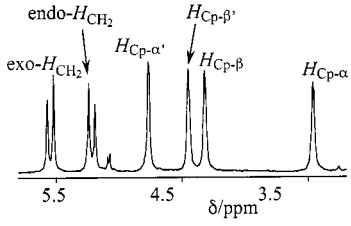

Figure 4. Methylene and cyclopentadienyl region of the ^1H NMR spectrum of $[HgL^1](CF_3SO_3)_2$ at room temperature in CD_3CN

CV experiments have confirmed that one Hg^{II} ion is complexed with one L^1 ligand. The addition of increasing amounts of $Hg(CF_3SO_3)_2$ to a solution of L^1 in acetonitrile results in the growth of a new Fc/Fc^+ wave ($E_{1/2}$ = 0.68 V) weakly separated from the original Fc/Fc^+ wave. This wave reaches full development after the addition of one mol equivalent of mercury salt and replaces the original Fc/Fc^+ wave in free L^1 (Figure 5A). In addition, the $[HgL^1]^{2+}$ complex presents an irreversible one-electron reduction wave (E_p = −0.75 V; Figure 5B), followed by several ill-behaved reduction peaks around −1.6 V. Reduction of the complex down to −2 V led to dissociation with formation of mercury metal, as evidenced on the reverse scan by the rise of a sharp mercury metal stripping peak (E_p = 0.42 V). The electrochemical behavior of $[HgL^1]^{2+}$ is summarized in Equation (4).

$$[Hg^{I}\mathbf{L^1}]^{+} \underset{+e}{\overset{-0.75\ V}{\rightleftharpoons}} [Hg^{II}\mathbf{L^1}]^{2+} \underset{+e}{\overset{0.68\ V}{\rightleftharpoons}} [Hg^{II}(\mathbf{L^1})^{+}]^{3-} \quad (4)$$

Electrochemical Behavior and Complexation of L^2 with Fe^{II}, Ni^{II} and Hg^{II}

Electrochemical Behavior and Polymerization of L^2

The CV behavior of L^2 in acetonitrile presents complex features. Repeated scans over the 0 to 1 V potential range (Figure 6A) leads to the progressive decrease of the Fc/Fc^+ redox wave ($E_{1/2}$ = 0.56 V) and to the rise of a large reversible peaks system ($E_{1/2}$ = 0.77 V; ΔE_p = 40 mV at ν = 0.1 Vs^{-1}). The new wave reaches full development when the original Fc/Fc^+ peak system has totally vanished (Figure 6A). This electroactivity is maintained after transfer of the electrode to clean CH_3CN + TBAP electrolyte and remains stable upon repeated scans (Figure 6B). This behavior is in accordance with the growth of an insoluble film of Fe-bis(terpyridine) complex onto the electrode surface. Indeed, the half wave potential of immobilized species is the same as that found for the $Fe^{II/III}$ couple in the $[Fe(L^2)]^{2+}$ complex ($E_{1/2}$ = 0.77 V; see Figure 6C and the discussion below) and is similar to that measured with the $[Fe(L^3)_2]^{2+}$ model complex ($E_{1/2}$ = 0.76 V) containing no ferrocenyl groups. The latter was obtained by in situ complexation of L^3 (Figure 1) with a half mol equivalent of Fe^{II}. Two broad, reversible waves (not shown in Figure 6) were also seen at −1.63 V and −1.82 V on the CV curve of the film, corresponding to ligand-localized reductions in the Fe-bis(terpyridine) moieties. These redox processes occur at −1.65 V and −1.80 V in the $[Fe(L^3)_2]^{2+}$ model complex.

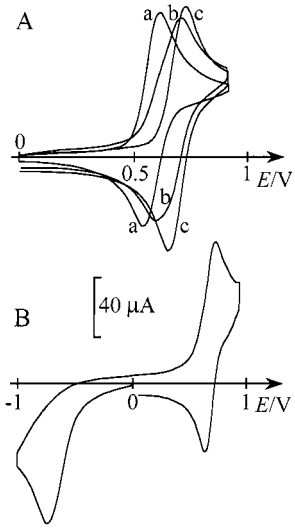

Figure 5. Cyclic voltammograms at a Pt disk electrode (5 mm diameter) in CH_3CN + TBAP 0.1 M: (A) (a) free L^1 (1.5 mM), (b) L^1 + 0.3 $Hg(CF_3SO_3)_2$, (c) L^1 + 1.0 $Hg(CF_3SO_3)_2$; (B) $[HgL^1](CF_3SO_3)_2$ 1.5 mM; scan rate 0.1 Vs^{-1}

The formation of Fe-bis(terpyridine) species upon oxidation of L^2 was corroborated by UV/Vis and FT-IR experiments. Around 40 scans have been performed in the 0 to 1 V potential range on a 1 cm^2 Pt electrode. The solution turned from orange to pink-violet and a dark-pink film covered the electrode surface. The visible spectrum of the electrolysis solution showed a new absorption peak at 557 nm, very close to that observed with the isolated $[FeL^2](ClO_4)_2$ complex (λ_{max} = 558 nm). Furthermore, the infrared spectrum of the film was characterized by strong bands at 1707 cm^{-1} (C=O stretching vibration) and 1628 cm^{-1} (terpyridine ring stretching vibration). These bands appear at 1708 and 1621 cm^{-1} in the $[FeL^2](ClO_4)_2$ complex.

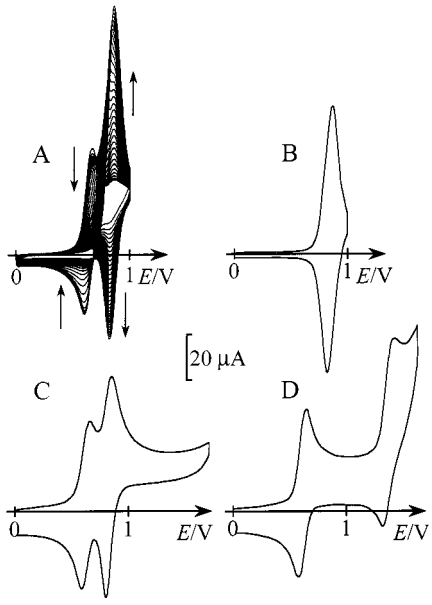

Figure 6. (A) Oxidative coating of a Pt disk electrode (5 mm diameter) with an Fe-bis(terpy) film, by repeated scans in a solution of L^2 (2.5 mM) in CH_3CN + TBAP 0.1 M; (B) modified electrode prepared in (A) and transferred to L^2-free CH_3CN + TBAP 0.1 M; (C) L^2 (2.5 mM) + 1 equiv. $Fe(ClO_4)_2$; (D) L^2 + 1 equiv. $Ni(ClO_4)_2$; scan rate 0.1 V

A similar behavior has already been observed with a ferrocenyl-substituted terpyridine containing an olefinic linkage.[4f] The formation of a polymer film containing iron centers in a terpyridine environment was attributed to the oxidative electropolymerization of the vinyl or vinyl-cyclopentadienyl backbone, followed by rupture of the ferrocenyl groups and complexation of iron cations. Since L^2 does not contain any olefinic group, the formation of a stable Fe-bis(terpyridine) material must be explained in a different way. Fe-bis(terpyridine) films are also obtained when the scan range is restricted to the Fc/Fc^+ redox couple. However, the films formed in these experimental conditions are of smaller size than those obtained when the potential scan range is extended up to 1 V. Electrode coating can thus be explained by considering the decomposition of the ferricinium groups in the presence of terpyridine ligands, to form poorly soluble Fe-bis(terpyridine) species, which precipitate onto the electrode surface. The high stability of the films upon cycling and their better growth when the scan range is increased up to 1 V could be due to some oxidative polymerization of free cyclopentadienyl groups released by decomposition of the ferricinium species.

The effect of added metal cations on film growth confirmed that this process is mainly due to the decomplexation of ferricinium groups by terpyridine ligands. The addition of small amounts (e.g. 0.2 mol equivalent) of Fe^{II}, Ni^{II} and Hg^{II} cations led to stabilization of the Fc/Fc^+ redox couple and slowed down the growth of the Fe-bis(terpyridine) films. This last process was fully inhibited in the presence of one mol equivalent of metal cation, suggesting the formation of 1:1 L^2 + M^{II} complexes (M = Fe, Ni, Hg).

The CV curves recorded in L^2 solutions containing one mol equivalent of metal cation show stable Fc/Fc^+ redox peak systems (Figure 6C and 6D). Complexation of L^2 with Fe^{II} ions is also revealed by the appearance of a $Fe^{II/III}$ redox wave ($E_{1/2}$ = 0.77 V; Figure 6C). The sharp and symmetrical shape of the Fe^{III} Fe^{II} reduction peak indicates that the oxidized form of the iron complex ($[FeL^2]^{4+}$) is poorly soluble in CH_3CN, adsorbs at the electrode surface during the scan towards positive potentials and dissolves upon reduction. No accumulation of complex onto the electrode surface was observed upon repeated scans. This observation confirms that the polymerization of free cyclopentadienyl groups is involved in the growth of films by oxidation of L^2.

Complexation of L^2 with Ni^{II} ions is also evidenced by the rise of a $Ni^{II/III}$ redox wave at 1.31 V (Figure 6D). This wave was found at 1.33 V for the $[Ni(L^3)_2]^{2+}$ model complex. No redox system concerning the metal centre could be found with the $[HgL^2]^{2+}$ complex. As already observed for other complexes of ferrocene-functionalized terpyridines,[4a,4f,4g] the potential of the Fc/Fc^+ process is slightly or not changed upon complexation of L^2 (+10 mV, +5 mV and 0 mV for Hg^{II}, Ni^{II} and Fe^{II} complexes, respectively). This behavior contrasts with that obtained upon complexation of the phen-based ligand L^1. As already found with iron,[7c] nickel and mercury complexes of L^1, the drop in the ν(CO) stretching vibration in L^2-based complexes (see the Exp. Sect.) indicates a coordination between the metal center and the oxygen atoms of the carbonyl groups. However, this interaction is not sufficient to produce an appreciable electronic coupling between the ferrocene group and the metal center in complexes of L^2. Although we have no clear explanation at the present time, this different behavior could be due to a structural effect, since the ferrocenyl group is linked to very different positions with regard to the complexing site in L^1 (2-position) and in L^2 (4′-position). Complexation of L^1 may lead to a non-coplanarity of the Cp rings in the complexes, which is known to result in marked positive potential shifts in strained ferrocene derivatives.[9,10]

Finally, the formation of 1:1 L^2 + M complexes (M = Fe, Ni, Hg) was confirmed by FAB-MS measurements. The spectra of the isolated complexes only displayed peaks corresponding to $[\{ML^2\}X]^+$ entities (Fe and Ni: X = ClO_4^-; Hg: X = $CF_3SO_3^-$), without any evidence for the presence of oligomeric species.

Conclusion

This study confirms the remarkable complexation and electrochemical properties of polypyridyl-ferrocene metallosynthons towards various transition metal cations. Complexation of the 1,1′-bis(phen) derivative of ferrocene (L^1) with Cu^I, Ni^{II}, Fe^{II} and Hg^{II} cations results in large potential shifts of the ferrocenyl-centered redox process. This redox ligand could thus be used for the electrochemical recognition of selected metal cations. In contrast, complexation of the ferrocene-bis(terpy) derivative L^2 does not

alter appreciably the electron density on the ferrocenyl groups. Additionally, we found that the oxidative decomposition of L^2 is a simple way to tailor stable polymer films of Fe-bis(terpyridine) complexes.

Experimental Section

Reagents, Instrumentation and Procedure: Acetonitrile (Rathburn, HPLC grade) was used as received. Dichloromethane was dried over neutral alumina (activity I) for at least six days before use. Tetra-*n*-butylammonium perchlorate (TBAP) was purchased from Fluka and dried under vacuum for three days at 80 °C. Electrochemical experiments were conducted in a conventional three-electrode cell under an argon atmosphere at 20 °C. The reference electrode was $Ag/AgNO_3$ (10 mM in CH_3CN containing 0.1 M TBAP). The ferrocene/ferricinium (Fc/Fc^+) redox couple was used as internal standard. FAB (positive mode) mass spectra were recorded with an AEI Kratos MS 50 spectrometer fitted with an Ion Tech Ltd. gun and using *m*-nitrobenzyl alcohol as matrix. Elemental analysis were performed by the Service Central d'Analyses, CNRS, Lyon.

Ligands: L^1 was synthesized as previously reported.[7c] ^1H NMR (250 MHz, CD_3CN): δ = 2.76 (s, 6 H, CH_3), 4.52 (t, 4 H, $H_{\beta\beta'}$), 4.91 (t, 4 H, $H_{\alpha\alpha'}$), 5.52 (s, 4 H, CH_2), 7.49 (d, J = 7.9 Hz, 2 H, H_8), 7.60−7.83 (m, 6 H, $H_{5,6,3}$), 8.13 (d, J = 7.9 Hz, 2 H, H_7), 8.23 (d, J = 7.9 Hz, 2 H, H_4). FAB-MS: m/z = 687 $[L^1 + H]^+$. UV/Vis (d-d band; CH_3CN): λ_{max} (ε/M^{-1} cm^{-1}) = 450 nm (300). FT-IR (KBr): ν(CO) = 1713 cm^{-1}. $C_{40}H_{30}FeN_4O_4$ (686.16): C 69.88, H 4.40, N 8.16; found C 69.26, H 4.89, N 8.36.

L^2 was prepared by the stoichiometric reaction of 4′-(hydroxymethyl)-2,2′:6′,2"-terpyridine[11] with 1 mmol of 1,1′-bis(chlorocarbonyl)ferrocene[12] in 10 mL of dried toluene containing 4 mmol of freshly distilled triethylamine. The reaction mixture was stirred overnight under an inert atmosphere, then filtered and the solvents evaporated to dryness. The crude product was extracted with CH_2Cl_2 and the organic phase was washed with H_2O. The solvent was removed in vacuo and the crude product was purified by column chromatography on neutral alumina eluting with CH_2Cl_2, to yield L^2 (70%) as an orange solid. ^1H NMR (250 MHz, CD_3CN): δ = 4.52 (t, 4 H, $H_{\beta\beta'}$), 5.08 (t, 4 H, $H_{\alpha\alpha'}$), 5.40 (s, 4 H, CH_2), 7.30 (dd, J = 7.5, 4.8 Hz, 4 H, $H_{5,5''}$), 7.79 (td, J = 7.7, 1.6 Hz, 4 H, $H_{4,4''}$), 8.45 (s, 4 H, $H_{3',5'}$), 8.55 (d, J = 7.9 Hz, 4 H, $H_{3,3''}$), 8.65 (m, 4 H, $H_{6,6''}$). FAB-MS: m/z = 765 $[L^2 + H]^+$. UV/Vis (d-d band; CH_2Cl_2): λ_{max} (ε/M^{-1} cm^{-1}) = 453 nm (310). FT-IR (KBr): ν(CO) = 1718 cm^{-1}. $C_{44}H_{32}FeN_6O_4{\cdot}H_2O$ (782.65): C 67.53, H 4.38, N 10.74; found C 67.51, H 4.34, N 10.24.

Complexes: The quantitative synthesis of metal complexes (yield 90%) was performed by the reaction of stoichiometric amounts of L^1 or L^2 and a metal salt {$[Cu(CH_3CN)_4]ClO_4$, $[Ni(ClO_4)_2{\cdot}xH_2O]$, $[Fe(ClO_4)_2{\cdot}6H_2O]$ and $[Hg(CF_3SO_3)_2]$} at room temperature in CH_2Cl_2. Products were precipitated by the addition of diethyl ether and collected by suction filtration. **Warning**! *Perchlorate salts are hazardous because of the possibility of explosion*. Characterization of the $[FeL^1](ClO_4)_2$ complex has already been reported.[7c]

$[CuL^1]ClO_4$: ^1H NMR (250 MHz, CD_3CN): δ = 2.56 (s, 6 H, CH_3), 3.66 (s, 2 H, H_α), 4.37 (s, 2 H, H_β), 4.43 (s, 2 H, $H_{\beta'}$), 4.72 (s, 2 H, $H_{\alpha'}$), 4.88 (d, J = 12.0 Hz, 2 H, CH_2-endo), 5.47 (d, J = 12.0 Hz, 2 H, CH_2-exo), 7.90 (d, J = 7.9 Hz, 2 H, H_8), 8.17 (d, J = 2.4 Hz, 4 H, $H_{5,6}$), 8.28 (d, J = 7.9 Hz, 2 H, H_3), 8.63 (d, J = 7.9 Hz, 2 H, H_7), 8.73 (d, J = 7.9 Hz, 2 H, H_4). FAB-MS: m/z = 749 $[CuL^1]^+$. UV/Vis (CH_3CN): λ_{max} (ε/M^{-1} cm^{-1}) = 444 nm (6975). FT-IR (KBr): ν(CO) = 1713 cm^{-1}. $C_{40}H_{30}ClCuFeN_4O_8{\cdot}H_2O$ (867.57): C 55.38, H 3.72, N 6.46; found C 55.45, H 3.54, N 6.76.

$[HgL^1](CF_3SO_3)_2$: ^1H NMR (250 MHz, CD_3CN): δ = 3.01 (s, 6 H, CH_3), 3.47 (s, 2 H, H_α), 4.32 (s, 2 H, H_β), 4.45 (s, 2 H, $H_{\beta'}$), 4.77 (s, 2 H, $H_{\alpha'}$), 5.22 (d, J = 12.0 Hz, 2 H, CH_2-endo), 5.54 (d, J = 12.0 Hz, 2 H, CH_2-exo), 8.21 (d, J = 7.9 Hz, 2 H, H_8), 8.35 (d, J = 2.2 Hz, 4 H, $H_{5,6}$), 8.46 (d, J = 7.9 Hz, 2 H, H_3), 8.92 (d, J = 7.9 Hz, 2 H, H_7), 9.06 (d, J = 7.9 Hz, 2 H, H_4). FAB-MS: m/z = 1037 $[\{HgL^1\}CF_3SO_3]^+$. UV/Vis (CH_3CN): λ_{max} (ε/M^{-1} cm^{-1}) = 454 nm (360). FT-IR (KBr): ν(CO) = 1710 cm^{-1}. $C_{42}H_{30}F_6FeHgN_4O_{10}S_2$ (1185.3): C 42.56, H 2.55, N 4.73; found C 42.43, H 2.37, N 4.33.

$[NiL^1](ClO_4)_2$: FAB-MS: m/z = 843 $[\{NiL^1\}ClO_4]^+$. UV/Vis (CH_3CN): λ_{max} (ε/M^{-1} cm^{-1}) = 454 nm (450). FT-IR (KBr): ν(CO) = 1664 cm^{-1}. $C_{40}H_{30}Cl_2FeN_4NiO_{12}{\cdot}H_2O$ (962.17): C 49.93, H 3.35, N 5.82; found C 49.23, H 3.28, N 6.06.

$[HgL^2](CF_3SO_3)_2$: FAB-MS: m/z = 1115 $[\{HgL^2\}CF_3SO_3]^+$. No correct elemental analysis for this compound could be obtained.

$[NiL^2](ClO_4)_2$: FAB-MS: m/z = 921 $[\{NiL^2\}ClO_4]^+$. UV/Vis (CH_3CN): λ_{max} (ε/M^{-1} cm^{-1}) = 452 nm (496). FT-IR (KBr): ν(CO) = 1666 cm^{-1}. $C_{44}H_{32}Cl_2FeN_6NiO_{12}{\cdot}H_2O$ (1040.2): C 50.08, H 3.29, N 8.08; found C 49.82, H 3.23, N 7.73.

$[FeL^2](ClO_4)_2$: FAB-MS: m/z = 919 $[\{FeL^2\}ClO_4]^+$. UV/Vis (CH_3CN): λ_{max} (ε/M^{-1} cm^{-1}) = 558 nm (2150), 510 (1050, sh). FT-IR (KBr): ν(CO) = 1708, 1621 cm^{-1}. $C_{44}H_{32}Cl_2Fe_2N_6O_{12}{\cdot}H_2O$ (1037.4): C 50.94, H 3.30, N 8.10; found C 50.75, H 3.25, N 8.01.

[1] A. Harriman, R. Ziessel, *Chem. Commun.* **1996**, 1707−1716.
[2] A. M. DeBlass, C. DeSantis, L. Fabbrizzi, M. Licchelli, P. Pallavicini, A. Poggi, in *Supramolecular Chemistry* (Eds.: V. Balzani, L. DeCola), Kluwer Academic Publishers, London **1995**, 87−103.
[3] [3a] P. D. Beer, O. Kocian, R. J. Mortimer, *J. Chem. Soc., Dalton Trans.* **1990**, 3283−3288. [3b] I. R. Butler, *Organometallics* **1992**, *11*, 74−83. [3c] I. R. Butler, N. Burke, L. J. Hobson, H. Findenegg, *Polyhedron* **1992**, *19*, 2435−2439. [3d] B. König, M. Nimtz, H. Zierg, *Tetrahedron* **1995**, *22*, 6267−6272. [3e] N. Sachsinger, C. D. Hall, *J. Organomet. Chem.* **1997**, *531*, 61−55. [3f] S. Achar, C. E. Immoos, M. G. Hill, V. J. Catalano, *Inorg. Chem.* **1997**, *36*, 2314−2320.
[4] [4a] J.-C. Chambron, C. Coudret, J.-P. Sauvage, *New. J. Chem.* **1992**, *16*, 361−367. [4b] B. Farlow, T. A. Nile, J. L. Walsh, A. T. McPhail, *Polyhedron* **1993**, *23*, 2891−2894. [4c] E. C. Constable, A. J. Andrews, M. D. Marcos, P. R. Raithby, R. Martínez-Máñez, M. J. L. Tendero, *Inorg. Chim. Acta* **1994**, *224*, 11−14. [4d] E. C. Constable, A. J. Andrews, R. Martínez-Máñez, P. R. Raithby, A. M. N. Cargill Thompson, *J. Chem. Soc., Dalton Trans.* **1994**, 645−650. [4e] I. R. Butler, S. J. McDonald, M. B. Hursthouse, K. M. Abdul Malik, *Polyhedron* **1995**, *14*, 529−539. [4f] M. E. Padilla-Tosta, R. Martínez-Máñez, J. Soto, J. M. Lloris, *Tetrahedron* **1998**, *54*, 12039−12046. [4g] U. Siemeling, U. Vorfeld, B. Neumann, H.-G. Stammler, P. Zanello, F. Fabrizi de Biani, *Eur. J. Inorg. Chem.* **1999**, 1−5.
[5] E. C. Constable, R. Martínez-Máñez, A. M. W. Cargill Thompson, J. V. Walker, *J. Chem. Soc., Dalton Trans.* **1994**, 1585−1594.
[6] E. C. Constable, A. J. Edwards, R. Martínez-Máñez, P. R. Raithby, *J. Chem. Soc., Dalton Trans.* **1995**, 3253−3261.

[7] [7a] M. Buda, J.-C. Moutet, E. Saint-Aman, A. De Cian, J. Fisher, R. Ziessel, *Inorg. Chem.* **1998**, *37*, 4146−4148. [7b] M. Buda, J.-C. Moutet, A. Pailleret, E. Saint-Aman, R. Ziessel, *J. Electroanal. Chem.* **2000**, *484*, 164−171. [7c] A. Ion, J.-C. Moutet, E. Saint-Aman, G. Royal, S. Tingry, J. Pécaut, S. Ménage, R. Ziessel, *Inorg. Chem.* **2001**, *40*, 3632−3636. [7d]A. Ion, M. Buda, J.-C. Moutet, E. Saint-Aman, G. Royal, I. Gauthier-Luneau, M. Bonin, A. Harriman, R. Ziessel, submitted for publication.

[8] C. Dietrich-Buchecker, J.-P. Sauvage, J.-M. Kern, *J. Am. Chem. Soc.* **1989**, *111*, 7791−7800 and references therein.

[9] J. C Medina, T. T. Goodnow, M. T. Rojas, J. L. Atwood, A. E. Kaifer, G. K. Gokel, *J. Am. Chem. Soc.* **1992**, *114*, 10583−10595.

[10] H. Scholl, K. Sochaj, *Electrochim. Acta* **1991**, *36*, 689−694.

[11] M. E. Padilla-Tosta, J. M. Lloris, R. Martínez-Máñez, A. Benito, J. Soto, T. Pardo, M. A. Miranda, M. Dolores-Marcos, *Eur. J. Inorg. Chem.* **2000**, 741−748.

[12] J.-C. Moutet, E. Saint-Aman, M. Ungureanu, T. Visan, *J. Electroanal. Chem.* **1996**, *41*, 79−85.

Received September 7, 2001
[I01348]